

The Unexpected Consequences of a Small Side-Hill Fill

D.D. Dasenbrock

Minnesota Department of Transportation, Maplewood, Minnesota, USA

P.J. Axtell

Dan Brown and Associates, Sequatchie, Tennessee, USA

A.S. Budge

Minnesota State University, Mankato, Minnesota, USA

ABSTRACT: In late 2014, the Minnesota Department of Transportation repaired a highway embankment in Little Canada, MN. The embankment is 30-ft in height, and had been in operation for several decades, showing no signs of distress prior to a reconstruction project in 2006. As part of the 2006 corridor improvement project, additional fill was placed on the west side slope adjacent to the existing embankment section of interest. The modest amount of new fill caused unintended distress almost immediately after the new asphalt roadway shoulder was paved. Following construction, ongoing settlement and surface cracking in the asphalt shoulder required regular maintenance and patching. The recurring pavement distress and maintenance needs led to a remediation project, construction of which started in August of 2014. Plausible causes of the continued deformation were identified as: marginal embankment stability, low resistance to lateral squeeze, and consolidation under the stresses imposed by the embankment. The design challenge was to devise a successful remediation method capable of addressing all three possible sources of deformation. After considering several options, the preferred remediation employed a two-component solution using a cantilever HP18x135 soldier pile wall combined with slope unloading by soil removal. The solution addresses settlement, deformation, and embankment stability aspects of the site.

This paper describes the events leading to the embankment distress, the subsequent subsurface investigation, monitoring program, probable cause(s), design development and analysis, design selection, and construction considerations.

1 INTRODUCTION

In 2004, a 4-year long \$120 million dollar Minnesota state highway project was contracted to “Unweave the Weave” and improve traffic flow at the intersection of I-694 and I-35E, north of St. Paul, MN. The project consisted of the construction of numerous bridges and several roadway alignment changes as well as the construction of noise walls, storm water detention ponds, and other facilities. The Minnesota Department of Transportation (MnDOT) widened the connection ramp between eastbound I-694 and I-35E southbound in Little Canada, MN as part of the project work in 2006. Here, what was expected to be a routine embankment side-hill widening and flattening resulted in unexpected and unusual consequences along several hundred feet of roadway. Settlement of several inches and surface cracking in the asphalt shoulder occurred as construction in the area was taking place. It would later be discovered the embankment was situated above a deep deposit of compressible clayey soils and, in some places, a thin layer of compressed organic materials. Prior to that discovery, recurring pavement distress and the accompanying persistent regular maintenance needs led quickly to a more comprehensive geotechnical study of the area and the development of a remediation project, the construction for which was started in August of 2014 at a cost of about \$1.5M.

2 PROJECT BACKGROUND AND SITE INVESTIGATION

2.1 Project Background

The existing highway embankment for the connection ramp between eastbound I-694 and I-35E southbound was approximately 30-ft tall and had been in operation for several decades prior to the 2006-2008 grading and embankment construction. A new bituminous shoulder, concrete curb, and plate beam guardrail were added to the roadway section. This work required only a very narrow widening at the top of the western embankment. Although there were minor changes to the roadway grading, the elevation of the top of the embankment and pavement was essentially consistent with the in-place roadway geometry. Figure 1 shows the geometry of the existing slope and the new slope constructed during the project.

In the embankment section of interest, just to the south of Bridge 62914, the embankment base was designed for a widening of about 35 feet with a maximum amount of new fill of about 10 feet in height, being placed at the former embankment toe. This added fill was to flatten the slope from the in-place condition to create a 1V:3H slope. At some point, perhaps when the new fill began to encroach on a wetland area to the west, the extent of the fill appears to have been adjusted. The actual in-place fill is about one-half the intended design fill with a widening of only about 10 feet to 15 feet at the base with a corresponding maximum added height of about 5 feet. Prior to this project no signs of roadway distress had been documented. The modest amount of new side-hill fill began causing distress to the bituminous roadway shoulder at the top of the slope as the reconstruction project neared completion in the spring of 2008. A dip of several inches in the asphalt shoulder was observed shortly after it was placed, with large cracks extending from the Bridge 62914 approach panel area (the southern approach panel had not yet been placed) across the shoulder paving to the newly installed concrete curb.

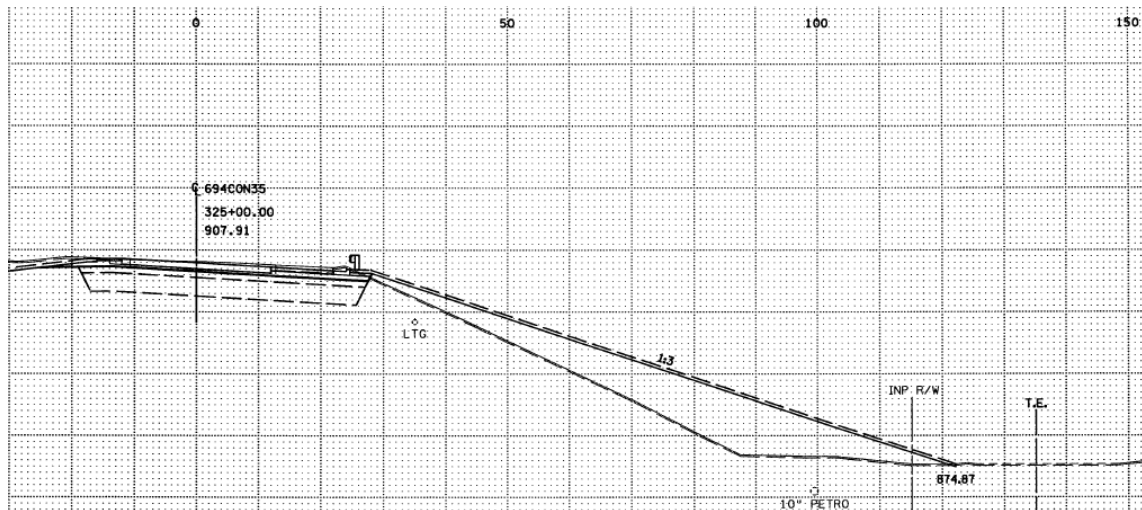


Figure 1. New construction widened the roadway embankment to the west. The toe was extended about 10 feet toward a wetland area flattening the existing slope to a 1H:3V condition. The actual fill placed during the project was only about half of the fill shown in the design drawing (shown).

Following the 2006-2008 construction activities, ongoing settlement and surface cracking in the asphalt shoulder required regular maintenance and patching to ensure safety to motorists. Each time more asphalt was added to the area to cover the cracks and fill in the depression, similar cracking and settlement would repeat. The recurring pavement distress and regular maintenance requirements led to the design of a remediation project in 2011; construction was started in August of 2014. Figure 2 shows the distress observed during construction in the spring of 2008 and subsequent distress, after multiple patching activities, in June of 2010.



Figure 2. Distress cracks in the bituminous shoulder were seen during construction shortly after the bituminous shoulder was placed (left) in April 2008. New distress is seen (right) in June 2010.

2.2 Site Investigation

When the asphalt settlement and related pavement cracking were observed by project inspectors, the MnDOT Foundations Office was contacted to perform a site investigation. A geotechnical investigation, which would eventually be conducted in several phases, began in April of 2008. The initial work consisted of 5 CPTu soundings. No near-surface cause of the distress could be immediately determined. Two soil borings were then advanced in May of 2008; slotted inclinometer casings were installed and the boreholes were subsequently used for traversing probe inclinometer measurements. One boring was located near the crest of the slope and the other at the base of the slope, both relatively close to the north end of the embankment where it tapered into the Bridge 62914 abutment end embankment.

Boring T1SI, advanced near the slope crest, showed predominantly granular materials with good bearing characteristics to a depth of 60 feet. From a depth of 60 feet to 66 feet, a very moist silty clay layer was encountered. Below that layer wet loamy and sandy soils were found to the depth of the boring at 85 feet. Boring T2SI, advanced near the toe of the widened slope showed very different conditions. Here, below about 10 feet of surface sandy soils a layer of organic materials was found to exist from a depth of 10 feet to a depth of 27 feet. The organic content of this material ranged from 12% to 42%. A soft silty-clay layer of soil was found immediately below this layer to a depth of nearly 50 feet. Loamy sandy soils, similar to those seen at boring T1SI were found below that layer from a depth of 50 feet to 65 feet. Three additional CPTu soundings were advanced in July of 2008; subsurface stratigraphy from the borings and the soundings was in good agreement both below the roadway shoulder, where the distress was occurring, and at the embankment toe. A very deep layer of apparently compressed clay existed below the embankment fill, and toward the western original grade the layer was thicker and extended closer to the ground surface. Here the soft layer was also overlain by a thick layer of compressible, low strength and high moisture content organic materials. These materials consisted of fibrous peat and peat with shells as well as organic silt loam.

Given the soil profile, it was not clear how the relatively deep soft and compressible layers could be influencing the behavior of the asphalt roadway shoulder; the embankment was constructed out of predominantly sandy soils with relatively good strength and there was no apparent distress to the nearby bridge, the bridge approach panels, or the concrete paving.

The two inclinometers would reveal within the first year of surveys that there was lateral movement both at the crest of the embankment and the embankment toe. In the first year of monitoring at T1SI, at the crest, movement of 2 inches was observed, originating at a depth of about 40 feet within the sandy loam material above the softer cohesive soils which were encountered at a depth of 60 feet below the roadway shoulder. Also in the first year of observation, inclinometer T2SI, at the toe of the embankment, also showed about 2 inches of cumulative

movement. Here, the deformation started at a depth of about 50 feet, which coincided with the depth of the soft silty clay soils.

Based on the subsurface material and stratigraphy information from the CPTu soundings and two boreholes, as well as the manual traversing probe inclinometer information, it was decided to expand the site investigation and install additional monitoring equipment. Slightly south of the initial investigation and on a cross section that was somewhat more centered on the area showing the greatest roadway distress, two additional boreholes were drilled in May and June of 2009. Similar to T1SI and T2SI, these borings were placed at the crest of the slope and at the base of the slope. After drilling and sampling, these borings were cased and two ShapeAccelArray (SAA) systems were installed. SAA systems are similar to in-place inclinometers and are described further by Danish (2008). A third SAA system became available from another project and was installed at the mid-slope after a third borehole was advanced four months later in November of 2009. The relative locations of the instrumented boreholes are shown in Figure 3.

The SAA sensor results agree with the traversing probe information and show that the embankment is slowly deforming and moving toward the west. In general the movement can be described as tilting rather than slipping; the upper soil layers appear to be deforming with small displacements throughout the embankment rather than shearing along a well-defined plane.



Figure 3. The embankment fill is shown looking southwest from the adjacent bridge. T1SI and T2SI are borings with slotted casing for manual traversing probe inclinometer use. Installations SAA11, SAA12, and SAA 16 are outfitted with automated ShapeAccelArray sensors.

2.3 Site Information Review and Interpretation

On the basis of the borings, laboratory tests, CPTu soundings, and recorded deformation data, several plausible causes of the continued deformation observed in the asphalt shoulder area of the in-situ instruments were identified. Causes were postulated as: marginal embankment stability; low resistance to lateral squeeze; bulk compression of peat and organic soils; and renewed consolidation of relatively deep subsurface materials under the new stress state imposed by the widened embankment. Given the geometry of the new fill and the apparent differences in the subsurface profile, differential movement appeared highly probable with more deformation likely to occur near the base of the embankment. It was also noted that each repair where more bituminous concrete was placed to build up the roadway shoulder was likely promoting the continued distress as the added material continued to increase the weight of the distressed area. Based on the stratigraphy, material properties, and observed behavior, it was determined that a site model should be developed and a slope stability analysis conducted to examine the existing behavior and evaluate possible mitigation strategies for their potential effectiveness.

3 SLOPE STABILITY ANALYSIS

Slope stability analyses were performed to assess the existing condition of a single, representative cross-section defined by the site geometry. The stratification and materials properties used in the model were established from the available boring logs and CPT soundings. Several remediation options were evaluated with respect to the existing condition. The two-dimensional limit-equilibrium slope stability software SLIDE (Rocscience, Inc.) was used. Only circular surfaces were considered to find the critical shear surface because continuous, weak, thin seams were not believed to exist based on the CPT soundings. Anisotropic shear strength behavior, while possible, was also not expected, and therefore not modeled in the analyses. External loads, such as traffic, were not included in the base model as transient loading induced by traffic was not believed to be a primary factor in the continued deformation of the slope. The addition of external load near the crest of the slope would reduce the computed factor of safety. A figure of the cross-section indicating the six different modeled strata is provided in Figure 4.

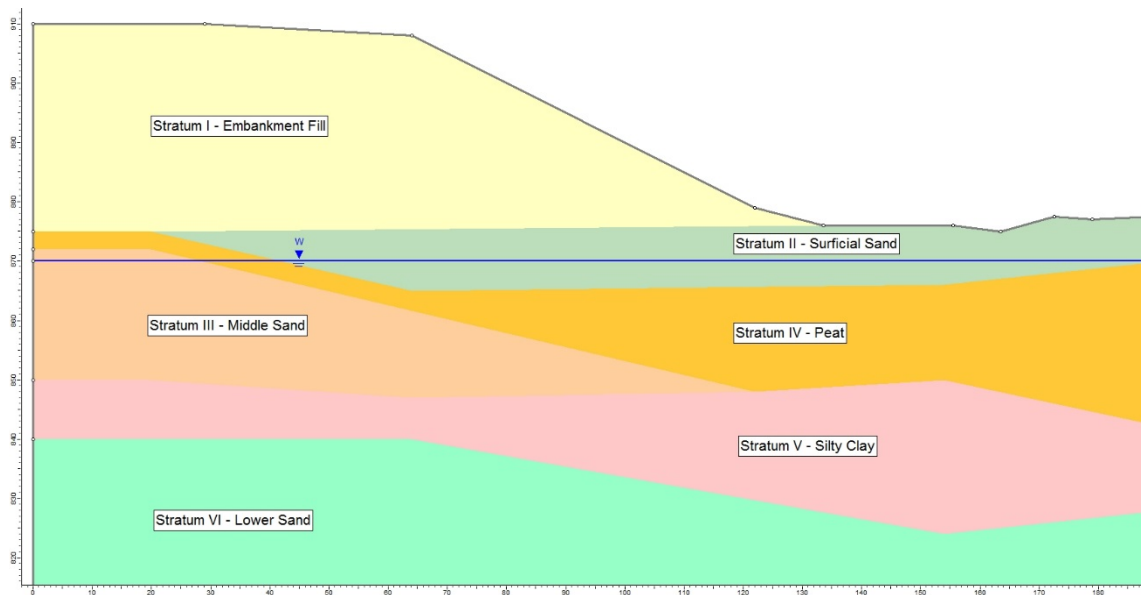


Figure 4. General Slope Stability Model Stratigraphy.

The soil properties used in the stability model are shown in Table 1. The shear strength, s , of the fine-grained soils (Strata IV and V) was modeled as a function of effective vertical stress, σ_v' . A s/σ_v' ratio equal to 0.2 was used for the highly organic peat in Stratum IV. Using that relationship and a value of 1,140 psf for σ_v' , the shear strength in the center of the 16 ft thick peat layer is estimated to be less than 250 psf. This value is consistent with estimates of s_u that can be made by dividing the measured tip resistance, q_c , from the CPTu soundings in the peat by an empirical factor equal to 17. The unconfined compression test results in Stratum IV indicated a higher undrained shear strength than expected based on CPTu data and experience with peat.

Similarly, a s/σ_v' ratio equal to 0.25 was used for the normally-consolidated silty clay in Stratum V. The s/σ_v' value in Stratum V generally agrees with the unconfined compression test results in that layer as reported on the boring logs. The shear strength and unit weight parameters for the coarse-grained soils in Strata I, II, III, and VI were estimated based SPT and CPTu results. The pore pressure was defined by a piezometric line at Elevation 870 ft.

Several slope stability analysis methods were considered: Bishop (Simplified), Janbu (Simplified), Janbu (Corrected), Spencer, Lowe and Karafiath, and GLE/Morgenstern and Price methods. These methods differ with respect to inter-slice force assumptions and, with the exception of Spencer's and Morgenstern and Price's methods, are statically indeterminate. Spencer's and Morgenstern and Price's methods are rigorous methods of slices that satisfy moment equilibrium in addition to force equilibrium and are believed to yield the most accurate results; the results of Morgenstern and Price's method are shown in Figure 5.

Table 1. Stability Model Soil Properties.

Stratum	Description	γ_t (pcf)	Shear Strength		
			c' (psf)	ϕ' (deg)	s/σ'
I	Embankment Fill	125	0	35	-
II	Surficial Sand	110	0	33	-
III	Middle Sand	125	0	35	-
IV	Peat	100	-	-	0.2
V	Silty Clay	105	-	-	0.25
VI	Lower Sand	125	0	38	-

Also shown in Figure 5 are the locations of two manual inclinometers, T1SI and T2SI (dashed lines), the critical shear circle determined from analysis of the existing condition, and the contour plot of the safety factor associated with the position of the trial radii. By inspection of the inclinometer displacement plots, good agreement exists between the predicted and measured location of the shear surface, supporting the appropriateness of the model for the existing condition. Distress cracking observed in the bituminous shoulder at the crest of the slope is also consistent with the critical shear surface, further supporting the model's parameters and results.

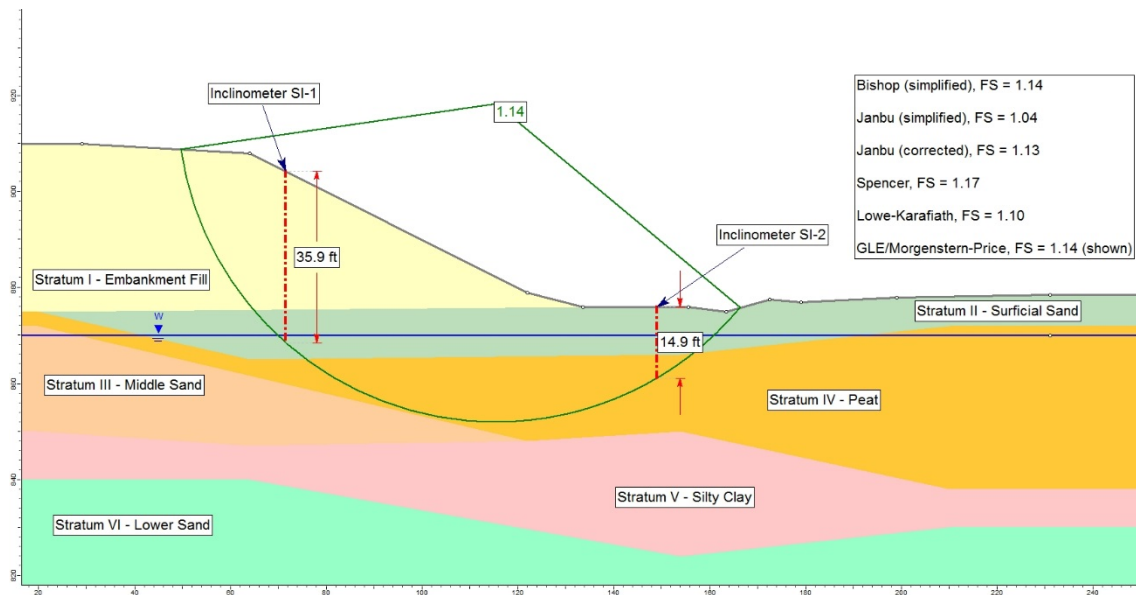


Figure 5. A Minimum Factor of Safety of 1.14 was obtained for the existing embankment condition based on the geometry and material parameters used to represent the site (for Morgenstern and Price's Method).

The multiple methods employed to search for critical surfaces produced a range of factors of safety; the relatively tight range and small standard deviation of the computed factors of safety provide confidence that the soil model is appropriate, as shown in Table 2.

Table 2. Minimum Slope Stability Factors of Safety.

Method of Slices	Minimum Factor of Safety
Bishop (Simplified)	1.14
Janbu (Simplified)	1.04
Janbu (Corrected)	1.13
Spencer	1.17
Lowe-Karafiath	1.10
GLE/Morgenstern-Price	1.14
Average	1.12
Standard Deviation	0.05

Results of these slope stability calculations indicate a marginally stable slope with a computed factor of safety of about 1.1. Therefore, utilizing a limit equilibrium approach, a failure (e.g., a factor of safety less than unity) is not predicted for the modeled conditions, consistent with the field conditions where a complete failure has not been observed. At low computed slope factors of safety, less than about 1.3, problematic deformations frequently occur. The minimum computed factors of safety from the soil models appear consistent with the ongoing deformation.

4 LATERAL SQUEEZE

The potential for lateral squeeze induced in the Stratum IV peat zone was evaluated. The increase in vertical stress applied by the 32 ft tall embankment fill slope may result in a factor of safety against lateral squeeze (FS_{SQ}) of less than 1.0 in the peat zone. The FS_{SQ} was computed using FHWA (2006) as follows:

$$FS_{SQ} = \left\{ \frac{(2)(s_u)}{[(\gamma)(D_s)(\tan \theta)]} \right\} + \left\{ \frac{(4.14)(s_u)}{[(\gamma)(h)]} \right\}$$

where s_u = undrained shear strength of soft soil beneath fill = varies based on s/σ ratio
 γ = unit weight of the fill = 125 lb/ft³
 D_s = depth of peat layer = 16 ft (varies, 16ft under lower 1/3 of slope)
 θ = angle of slope = 26.6° (2H:1V)
 h = height of fill = 32 ft (new fill thickness)

The s_u and D_s values of the Stratum IV peat vary. FS_{SQ} is inversely related to D_s . A D_s value equal to 16 ft was deemed appropriate because that is the thickness of the peat zone beneath the lower third of the slope. Towards the crest of the slope, D_s decreases, but beyond the toe, D_s increases. FS_{SQ} is directly and linearly related to s_u . As a means of evaluating the possible range of s_u and its effect on FS_{SQ} , Figure 6 was developed showing FS_{SQ} as it relates the s_u for selected slope angles.

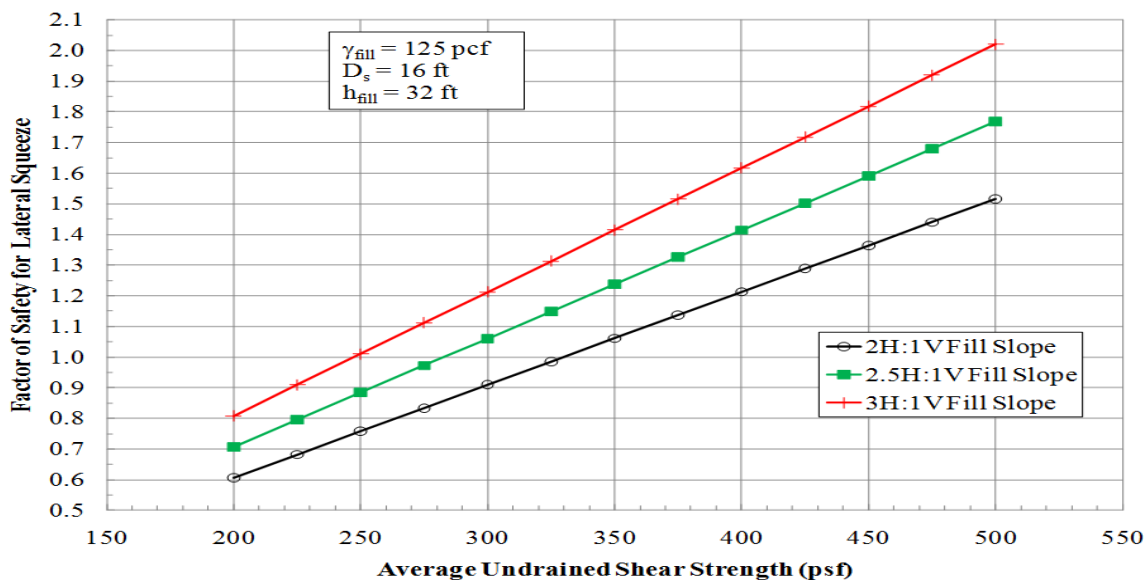


Figure 6. Stratum IV Peat Lateral Squeeze Evaluation Chart

The 2H:1V data series indicates that for FS_{SQ} equal to unity, s_u is about 330 psf, noting when FS_{SQ} approaches unity intolerable deformation should be anticipated. The 2H:1V data series indicates that for FS_{SQ} equal to 1.3, s_u is about 430 psf. The average s_u in the peat may be low; more likely the peat itself is not particularly stiff leading to bulk deformation and lateral squeeze as a second probable mechanism promoting the observed deformation.

It is recognized that the equation to estimate the factor of safety with respect to lateral squeeze is simplified and does not fully capture the complex nature of the phenomenon. In par-

ticular, only the undrained shear strength, or short-term conditions are evaluated. The continued nature of the deformation is likely the result of horizontal and vertical consolidation. Due to the predominantly fine-grained nature of some of the foundation soils, it is anticipated that deformations will continue to occur over a long time period. Secondary compression of the organic peat zone is expected to lengthen the duration.

5 FAILURE SUMMARY AND REMEDIATION CONCEPT

Based on the site investigation and analysis, causes for the continued deformation of the slope appear to be marginal embankment stability, low resistance to lateral squeeze, and consolidation under the stresses imposed by the embankment. Without correction, it was anticipated that unacceptable deformations may continue for an extended period of time and will require on-going maintenance; continuing to add corrective pavement patches may also serve to promote distress by successively adding new weight at the crest of the slope. Remediation methods addressing all three possible sources of deformation were desired as the distress was likely a composite result of these mechanisms. Several remedial options were evaluated, including lightweight fills, retaining walls, and column supported embankments. In performing concept-phase designs, several preliminary options were dismissed due to technical deficiencies or the inability to address all potential deformation sources. The final technical concept was developed based on a general economic evaluation and ability to address all potential deformation mechanisms.

The recommended remedial design is a permanent soldier pile and lagging retaining wall constructed at the crest of the slope. Down-slope of the retaining wall, the embankment fill is to be graded to a 1V:2.25 H slope. This approach unloads the foundation soils by removing the load induced by the embankment widening constructed in 2008, thereby addressing potential consolidation and lateral squeeze deficiencies. The cantilevered soldier pile and lagging retaining wall supports the roadway and also increases the limit equilibrium slope stability factor of safety for the highway embankment to an acceptable level.

The soldier piles were designed to resist a 12 ft retained height; to accommodate potential erosion or other unknown occurrences, the retained height was constructed as 9 ft (e.g., a 9 ft cut at the crest of the slope).

Although, permanent tie-backs were evaluated for use, allowing the use of a smaller soldier pile section, this option was dismissed for the following reasons: 1) the potential for continued axial deformation and subsequent unloading of the ties; 2) the requirement for corrosion protection considering the permanent nature of the retaining wall; and 3) the potential interference of the ties and walers with a wall facade or aesthetics.

6 SOLDIER PILE DESIGN

The soldier piles were designed using LPILE (Ensoft, Inc). The recommended soldier piles were HP18x135 sections embedded 78 ft beneath the crest of the slope and spaced on 5 ft center-to-center spacing. The 78 ft length was used to allow an 80 ft member, which is a typical length, and some stick-up for pile driving and possibly inclusion in a crash wall.

The HP18x135 has a moment of inertia about the strong axis of $2,196 \text{ in}^4$, a cross-sectional area of 39.8 in^2 , a depth of 17.5 in and a flange width of 17.75 in. These relatively large sized piles at a 5 ft center-to-center spacing provide more than enough resistance with respect to the retaining wall, but were necessary when considering global slope stability. An active earth pressure coefficient of 0.3 was used to estimate the horizontal load acting on the wall. A triangular stress distribution resulting from the active soil wedge over a 5 ft length (center-to-center pile spacing) was determined for use in LPILE and applied to the pile over the 12 ft cantilever wall height. In addition, a 250 psf uniformly distributed live load surcharge at the crest of the slope was also applied to replicate traffic loading according to FHWA guidelines. These two distributed loads were added together to simulate the lateral loading that the piles must resist.

The Active Earth Pressure (AEP) varied linearly from zero at the pile head to a maximum value at a depth of 12ft. The maximum magnitude of AEP was determined at the Service Limit State (SER) and Strength I Limit State (STR I):

$$AEP_{SER} = 2,250 \text{ lb/ft} = \underline{187.5 \text{ lb/in}} \quad ; \quad AEP_{STR I} = 3,375 \text{ lb/ft} = \underline{281.3 \text{ lb/in}}$$

The Live Load (LL) surcharge results in a rectangular, uniform stress distribution acting from the pile head to a depth of 12ft. The magnitude of LL was determined at the Service Limit State (SER) and Strength I Limit State (STR I) using the Load Factors recommended by AASHTO (2010):

$$LL_{SER} = 375 \text{ lb/ft} = \underline{31.3 \text{ lb/in}} \quad ; \quad LL_{STR I} = 656 \text{ lb/ft} = \underline{54.7 \text{ lb/in}}$$

At the Service Limit State, the combined trapezoidal stress distribution varied from 31.3 lb/in at the pile head to 218.8 lb/in at a 12 ft. depth. At the Strength I Limit State, the combined trapezoidal stress distribution varied from 54.7 lb/in at the pile head to 336.0 lb/in at 12 ft. depth.

Deflection of the wall was checked at the Service Limit State. The maximum computed deflection at the pile head (top of wall) was less than 1.5 inches for a 12 ft retaining wall height when subjected to the Service Limit State stress distribution. Assuming sound construction, this maximum computed deflection was considered to be an upper bound value. In addition, some of the deflection was expected during construction of the retaining wall; the post construction deflection for a 9 ft retaining wall was estimated to be minor for the purposes of a roadway.

The bending moment and shear induced in the soldier piles was checked at the Strength I Limit State. The maximum predicted bending moment in the pile is about 3,400 in-k for a 12 ft tall retaining wall. The resistance factor in flexure according to AASHTO (2010) is 1.00. Assuming 50 ksi steel, the HP18x135 pile can resist a maximum bending moment of 12,549 in-k. The maximum factored bending moment was well below the factored resistance, for 12 ft wall and 9 ft wall cases. The maximum predicted shear in the pile is about 29 k for a 12 ft tall retaining wall. The resistance factor in shear according to AASHTO (2010) is 1.00. Again assuming 50 ksi steel, the HP18x135 pile provides ample shear resistance.

Considering the permanent nature of the retaining wall and the excess moment and shear capacity of the pile section compared to the demand, loss of section resulting from corrosion could easily be accommodated and would not jeopardize the integrity of the wall.

7 REMEDIATED SLOPE STABILITY ANALYSIS

Global slope stability was analyzed for a 12 ft retained height using the soil properties established from evaluation of the existing condition. Those properties are provided in Table 1 and shown in Figure 7, along with the modeled geometry and layering. Note that modeling the shear strength in Stratum IV and V as a ratio of the effective vertical stress is slightly conservative considering an appreciable portion of the existing embankment will be excavated. The resulting reduction in effective vertical stress serves to reduce the shear strength beneath the excavated zone despite the fact that the soil now has been exposed to larger stresses. However, the minimum shear surfaces after remediation tend to develop in the embankment, so this slightly conservative modeling has little effect on the results of the analyses. The resistance provided by the HP18x135 soldier piles was manually included in the SLIDE analysis by determining the magnitude of shear force that can be mobilized in the piles. This mobilized shear force is primarily governed by geotechnical resistance as well as deflection of the pile and is substantially less than the shear capacity of the structural section. The magnitude of the mobilized shear was determined at several depths using the LPILE model under Service Limit State loading.

To determine the mobilized shear force at each depth interval in LPILE, the soil movement function was activated, which allows the pile to be loaded by moving soil at user-specified depth intervals. The amount of soil movement was set at 4 inches, which when applied to a depth of 57 ft beneath the pile head, resulted in the bending moment in the pile approaching the flexural capacity of the structural section. The resulting mobilized shear at a depth of 57 ft was 329 kips. When applied over the 5 ft center-to-center spacing, and for user-specified input into SLIDE, the shear resistance provided by the pile at that depth became 65.8 k/ft.

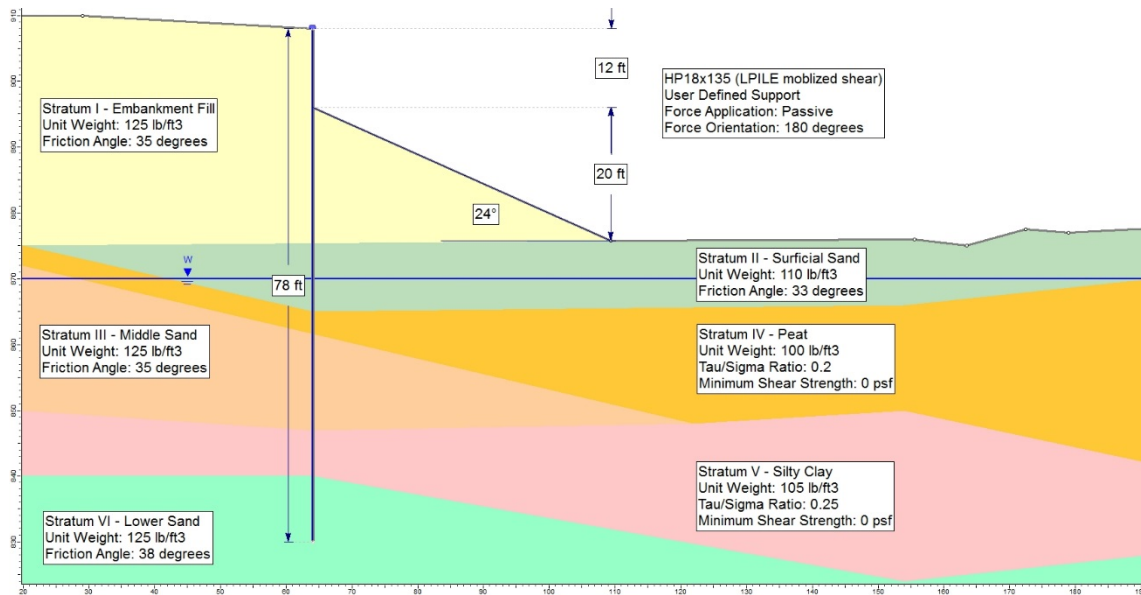


Figure 7. Slope stability model adapted to the mitigation strategy applying both soil unloading and a wall.

This same approach, including a constant 4 inch soil movement, was performed at several depths. The values were used in the SLIDE model at their respective depths after dividing by the 5 ft center-to-center spacing. Above the toe of the retaining wall, the mobilized shear used in SLIDE varied from zero at the pile head to the shear causing a pile head deflection of 4 inches. The resisting force provided by the mobilized shear was modeled as a passive resistance acting horizontally. Similar to the original stability assessment, only circular surfaces were considered; continuous, weak, thin seams were not seen in the CPTu data. Anisotropic shear strength behavior, while possible, is also not expected and therefore not modeled in these analyses.

Global stability was evaluated both for no external load and for a 250 psf live load (traffic) surcharge per FHWA guidelines. Stability was evaluated without the live load surcharge to quantify the increase in limit equilibrium slope stability provided by this remediation system as compared to the existing condition. Only the Spencer's and Morgenstern and Price's methods were used to analyze the remediated section as these methods are believed to yield the most accurate results, especially when including the soldier piles. Results of analyses using the Spencer's and Morgenstern and Price's methods are shown in Figure 8 for the live load surcharge case. Slope stability calculations indicate a stable slope with a computed factor of safety of about 1.5 under no external load, a substantial increase over the factor of safety for the existing condition of about 1.1. The minimum computed factor of safety under the 250 psf live load surcharge is about 1.3. Note that these factors of safety correspond to a 12 ft retained height, although a 9ft retained height was planned. Factors of safety were determined to be acceptable.

8 REMEDIATED LATERAL SQUEEZE ANALYSIS

The potential for lateral squeeze in the Stratum IV peat zone for the 23 ft tall, 2.25H:1V embankment fill slope was reevaluated and compared to the existing condition. With the exception of the slope height and angle of the remediated slope, the lateral squeeze parameters and equation were consistent with the analysis for the existing conditions. The factor of safety against lateral squeeze was found to increase more than 20% using the proposed remediation plan.

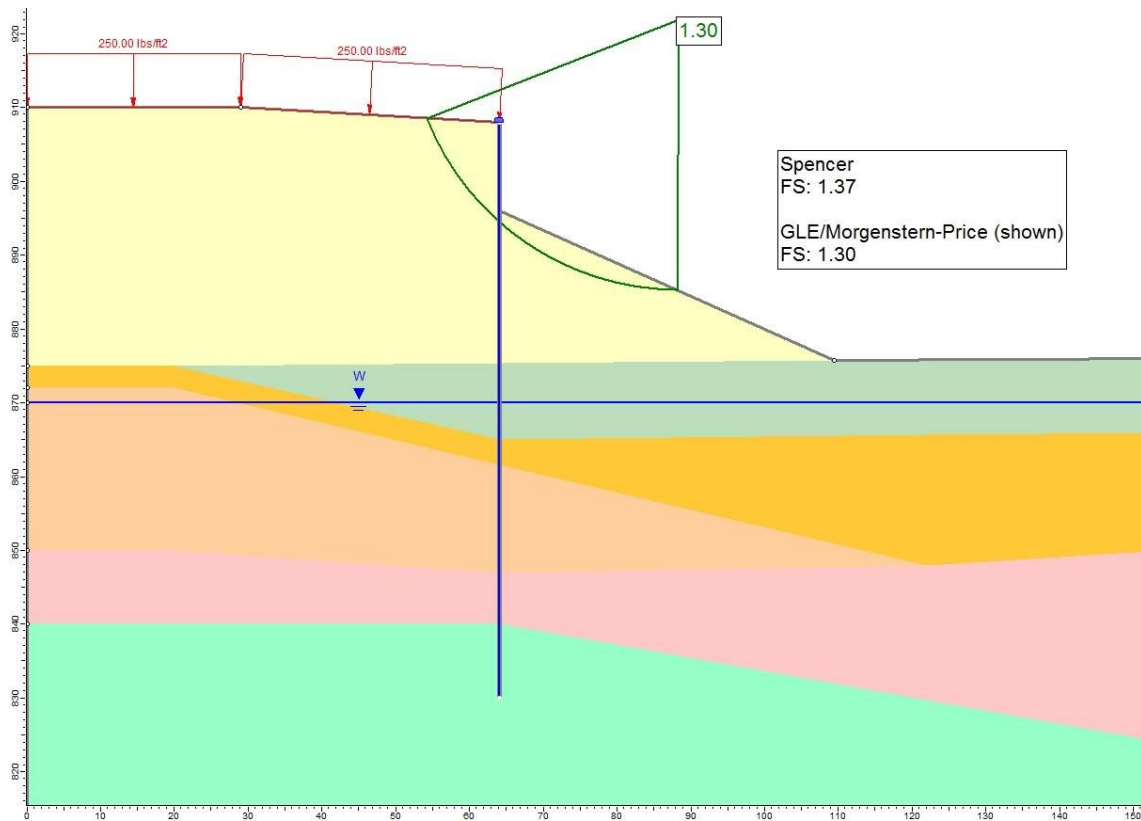


Figure 8. Global stability for remediated embankment section with 250 psf live load.

9 ADDITIONAL CONSIDERATIONS

The final wall design consisted of a coarse filter aggregate backfill placed behind the wall system. HP 18x135 soldier piles, on a 5 ft center-to-center spacing, were used with untreated timber lagging placed between the flanges of the pile elements. A minimum tip elevation for driving the piles was suggested to ensure that the piles were installed deep enough to meet design assumptions; little axial load will be imposed on the piles. Ten inches of structural concrete was placed for the outside wall; shear studs at one-foot spacing were placed along the exterior flange of the H-piles in the top 12 feet of the wall to help support the concrete. The piles were installed by mid-September 2014 (Figure 9); construction of the permanent concrete wall fascia was completed by the end of October 2014 (Figure 10).

As the condition of subgrade soils below the concrete mainline pavement was unknown and it was possible that voids might be present, coring was recommended. Although monitoring of the new wall system was suggested, it was not explicitly detailed and did not appear in the construction plans. Existing automated instrumentation was removed prior to construction to prevent it from being damaged; similar instrumentation may be reinstalled following the project as part of a performance monitoring program.

A geocomposite sheet drain was detailed for attachment to the back of the lagging; the lagging was to be embedded 6 inches into clean gravel fill. The clean gravel was to extend from the rear of the wall below the fascia and daylight at the front of the slope with a perforated pipe running through the gravel layer with lateral outlets. A drainage swale was recommended at the top of the wall. Discharge from the drainage systems was to be directed to appropriately protected spill slopes for erosion prevention. In the construction plans, 12 inch wide geocomposite strip drains were placed on the rear flanges of the piles and the swale and clean gravel layer were omitted. These detail changes represented deviations from the original design guidance, although the as-designed system meets the project intent, perhaps with somewhat less redundancy.



Figure 9. HP 18 x 135 piles were driven to provide stability to the roadway.



Figure 10. A ten inch thick permanent structural concrete wall was cast in front of the piles.

10 CONCLUSIONS

The ongoing deformation of the bituminous roadway shoulder was likely the result several, originally unforeseen, factors: marginal slope stability, vertical and horizontal consolidation under load induced by additional fill, and creep in peat and highly organic soils.

Regular pavement repairs were becoming costly; the site was investigated and remediation methods were evaluated. A solution capable of addressing all of the contributing factors was devised and constructed in the fall of 2014. The preferred remediation method used a hybrid solution consisting of the installation of an HP18x135 soldier pile wall combined with soil removal and slope unloading to address the identified failure mechanisms. The \$1.5M construction solution is expected to provide increased safety and reduced long-term maintenance costs. The project exemplifies how unfavorable geotechnical conditions can have significant cost implications.

11 REFERENCES

Danisch, L, Chrzanowski, A., Bond, J., and Bazanowski, M., [2008] Fusion of Geodetic and MEMS sensors for integrated monitoring and analysis of deformations, *Proceedings of the 13th FIG International Symposium on Deformation Measurements and Analysis / 4th IAG Symposium on Geodesy for Geotechnical and Structural Engineering*, May 12-15, Lisbon, Portugal.

FHWA (2006) *NHI-06-088, Soils and Foundations – Volume I*, December, 2006, Page 7-42.